Biosensors and Bioelectronics 39 (2013) 342–345

Contents lists available at SciVerse ScienceDirect

Biosensors and Bioelectronics

journal homepage: www.elsevier.com/locate/bios

Short communication

TiO_2 nanocrystals electrochemiluminescence quenching by biological enlarged nanogold particles and its application for biosensing

Shou-Nian Ding [a,*], Bu-Hong Gao [a], Dan Shan [b], Yue-Ming Sun [a], Serge Cosnier [c]

[a] School of Chemistry and Chemical Engineering, Southeast University, Nanjing 211189, China
[b] School of Environmental and Biological Engineering, Nanjing University of Science and Technology, Nanjing 210094, China
[c] Département de Chimie Moléculaire UMR-5250, ICMG FR-2607, CNRS Université Joseph Fourier, BP-53, 38041 Grenoble, France

ARTICLE INFO

Article history:
Received 24 May 2012
Received in revised form
16 July 2012
Accepted 30 July 2012
Available online 8 August 2012

Keywords:
TiO_2
Nanogold
ECL biosensor

ABSTRACT

Electrochemiluminescence (ECL) of TiO_2 nanocrystals with different crystal styles modified fluorine-doped tin oxide (FTO) electrode was investigated in H_2O_2 solution. The amorphous TiO_2 nanospheres were facilely synthesized by the hydrothermal and condensation method. Crystal TiO_2, namely anatase and rutile, were prepared by calcination of the amorphous TiO_2 nanospheres at 450 and 800 °C, respectively. The transmission electron microscope (TEM) and electron diffraction pattern were used to characterize the obtained TiO_2 nanoparticles morphology and the corresponding crystal styles. The electrochemical and ECL behaviors were investigated by cyclic voltammetry. The ECL quenching was observed by introduction of gold nanoparticles. Based on the quenching effect, a sensitive glucose ECL biosensor as a model was fabricated by in-situ growing-up gold seeds in $AuCl_4^-$ solution induced by biologically generated H_2O_2. The linear range to detect glucose is from 5.0×10^{-7} M to 4.0×10^{-3} M with the limit of detection of 2.5×10^{-7} M.

© 2012 Elsevier B.V. All rights reserved.

1. Introduction

Semiconductor nanocrystals (NCs) have been widely used in energy conversion, chemical analysis and clinical diagnosis for their rich, colorful, and unbleached excited emissions with narrow peak wavelength by controllable NCs species, crystal styles and sizes (Bruchez et al., 1998; Chan and Nie, 1998). In the past decade, electrochemiluminescence (ECL) of NCs have attracted great interest due to their potential applications in bioanalysis and luminescent devices (Liu et al., 2007; Zou and Ju, 2004; Ding et al., 2006; Shan et al., 2009, 2010a,b; Wu et al., 2011).

Upon the understanding of ECL mechanisms and the development of variety of coreactants, many new ECL systems of quantum dots (QDs) have been proposed by coreactant enhancing or signal quenching since the first ECL of Si QDs reported (Ding et al., 2002). Especially, IIB-VIA NCs' ECL have been intensively investigated in both organic and aqueous solutions due to their strong ECL intensities (Myung et al., 2002, 2004; Zheng et al., 2009; Poznyak et al., 2004; Bae et al., 2004; Ding et al., 2010). However, the inherent biotoxicity and instability limit their applications in a bioassay. Recently, many low-toxicity or nontoxic ECL species such as Au_{25} (Li et al., 2011), Ag nanocrystals (Diez et al., 2009), C-dots (Zheng et al., 2009), ZnO (Geng et al., 2007; Chen et al., 2011; Zhang et al., 2008) and TiO_2 nanostructures (Lin et al., 2008; Li et al., 2010; Liu et al., 2011) have also shown excellent ECL emission and have been used as ECL emitters.

Herein, the ECL behaviors of semiconductor TiO_2 nanoparticles modified FTO (fluorine-doped tin oxide) electrode with different crystal styles have been investigated in H_2O_2 solution. Interestingly, the ECL was quenched while gold nanoparticles were adsorbed upon the TiO_2 film. As reported, the nanogold seeds can grow up in $AuCl_4^-$ solution with the aid of H_2O_2 (Zayats et al., 2005; Xiao et al., 2004; Shlyahovsky et al., 2005; Pavlov et al., 2005). Meanwhile, H_2O_2 can be bio-generated by oxidase and its corresponding substrate. In the work, glucose oxidase (GOD) was used as a model enzyme to catalyze glucose oxidation to produce H_2O_2. Accordingly, an ECL biosensor was fabricated by the quenching effect using a bio-induced nanogold growth system to detect glucose in order to illustrate the potentialities of such ECL system for the development of optical DNA and protein sensors.

2. Experimental

2.1. Reagents

Fluorine-doped tin oxide (FTO) coated glass (NSG TEC™ C15, 14 Ω/sq resistance) prepared by a chemical vapor deposition process was purchased from Nippon Sheet Glass Co., Ltd. (Japan). All reagents used were commercially available and of analytical

* Corresponding author. Tel./fax: +86 25 52090621.
E-mail address: snding@seu.edu.cn (S.-N. Ding).

0956-5663/$ - see front matter © 2012 Elsevier B.V. All rights reserved.
http://dx.doi.org/10.1016/j.bios.2012.07.065

grade. Glucose oxidase (Aspergillus niger > 100 U/mg) was purchased from Shanghai Songon. Titanium isopropoxide (TTIP), Dodecylamine (DDA), Chloroauric acid tetrahydrate ($HAuCl_4 \cdot 4H_2O$), 3-mercaptopropionic acid (MPA) and Sodium borohydride ($NaBH_4$) were of analytical grade and obtained from Shanghai Chemical Plant. All aqueous solutions were prepared with doubly distilled water. Glucose solution was allowed to mutarotate at room temperature for 24 h before use.

2.2. Instruments

The electrochemical and ECL measurements were performed on an MPI-E analytical system (Xi'an Remex Analytical Instrument Ltd. Co.) at room temperature with an FTO working electrode ($1 \times 3\ cm^2$ with $1 \times 0.5\ cm^2$ for modification), a platinum counter electrode and a saturated calomel electrode (SCE). The detection window for ECL was placed in front of the photomultiplier tube (PMT) biased at 700 V. UV–visible absorption spectra were recorded using a Shimadzu UV3101 PC spectrophotometer. Emission spectra were recorded using a SLM-S8000 spectrofluorimeter. Transmission electron microscopy (TEM) images were performed on a transmission electron microscope (Philip CM-120).

2.3. Preparation of TiO_2 nanoparticles with different crystal styles

Titania particles were prepared by hydrolysis and condensation reaction of titanium isopropoxide (TTIP) with dodecylamine (DDA) as a catalyst in a co-solvent of methanol/acetonitrile (Tanaka et al., 2009). In a typical preparation, 0.18 ml water was added to 150 ml of methanol/acetonitrile solution. Then 0.28 g of DDA was dissolved in the mixture. After stirring for 10 min, 1 ml of TTIP was added and stirred for 8 h. Hydrolysis and condensation reaction were carried out providing a suspension of titania nano-spheres. Solid TiO_2 particles were cleaned by centrifugation, followed by drying at 60 °C. Antanase and rutile TiO_2 were obtained by calcination in 450 and 800 °C for 8 h, respectively.

2.4. Preparation of TiO_2 modified FTO electrodes

The suspension of TiO_2 (1 mg/mL) was prepared by dispersing amorphous, anatase and rutile TiO_2, respectively into water with the help of sonication for 30 min. A drop of 40 μL suspension of TiO_2 with different crystal styles was casted onto 1×0.5 cm FTO area, respectively, to prepare $TiO_{2\ amorphous}$/FTO, $TiO_{2\ anatase}$/FTO and $TiO_{2\ rutile}$/FTO electrodes. The modified electrodes dried at ambient atmosphere and kept in dark for use.

3. Results and discussion

3.1. Morphologies and crystal styles of TiO_2 and their ECL behaviors

TiO_2 crystal styles can be controllable by calcination. The morphologies of the prepared TiO_2 were characterized by TEM. As shown in Fig. 1(A), the prepared TiO_2 by hydrolysis and condensation are nano-spheres with the average diameter of ca. 250 nm. After the heat treatment at 450 °C, the size of the mean diameter of TiO_2 spheres decrease to ca. 200 nm, while the shape maintains. However, after calcination at 800 °C, the original sphere shape change to polyhedron. The phenomena were caused by the TiO_2 crystal style changing during the heat treatment. The insets of Fig. 1 show the selected-area electron diffraction (SAED) pattern of a single TiO_2 nanoparticle, which reveals the crystal nature of the obtained TiO_2 nanoparticle, namely (A) amorphous, (B) anatase and (C) rutile.

The electrochemical and ECL behaviors of TiO_2 nano-particles modified FTO electrodes with various crystal styles were investigated by cyclic voltammetry in 0.1 M PBS (pH 9) containing 10 mM H_2O_2. The ECL intensity was recorded simultaneously by PMT while the voltage scans cyclically from 0 to −1.5 V. The inset in Fig. 1 is cyclic voltammograms (CVs) of $TiO_{2\ amorphous}$/FTO (Curve a), $TiO_{2\ anatase}$/FTO (Curve b) and $TiO_{2\ rutile}$/FTO (Curve c) in 10 mM H_2O_2. As depicted in the inset, for the $TiO_{2\ amorphous}$/FTO, only one electrochemical process of reduction of H_2O_2 was exhibited during the voltage scan range (Curve a in the inset). However, another electro-reduction process was observed beyond −1.2 V after the reduction of H_2O_2 at both of $TiO_{2\ anatase}$/FTO (Curve b) and $TiO_{2\ rutile}$/FTO (Curve c), which is due to the electron injected into the TiO_2 crystals. The electrochemical properties of crystal TiO_2 and amorphous TiO_2 are coincident of their SAED patterns. Accordingly, the amorphous TiO_2 shows no ECL properties (Curve a) and the ECL only occurs at crystal TiO_2 modified electrodes (Curve b and c). Meanwhile, the ECL intensity at $TiO_{2\ rutile}$/FTO is about 1.5-folds larger than that of $TiO_{2\ anatase}$/FTO. And the voltage onsets of ECL are −1.16 V and −1.23 V for $TiO_{2\ rutile}$/FTO and $TiO_{2\ anatase}$/FTO, respectively. The larger ECL intensity and positively shift of voltage onset could be due to the better conductivity of rutile TiO_2 and more compact film formed with its polyhedron shape. Therefore, the $TiO_{2\ rutile}$/FTO was chosen for the following experiments (Fig. 2).

To obtain more information for the ECL mechanism of TiO_2, the electrochemical and ECL behaviors of $TiO_{2\ rutile}$/FTO were investigated in 0.1 M PBS with saturated nitrogen, saturated oxygen and 10 mM H_2O_2 (Fig. S1 in the supplemental information). The saturated nitrogen and oxygen solutions were prepared by purging nitrogen and oxygen, respectively into 0.1 M PBS for 30 min prior to use. In the saturated nitrogen solution, a reduction–oxidation redox process was observed beyond −1.0 V,

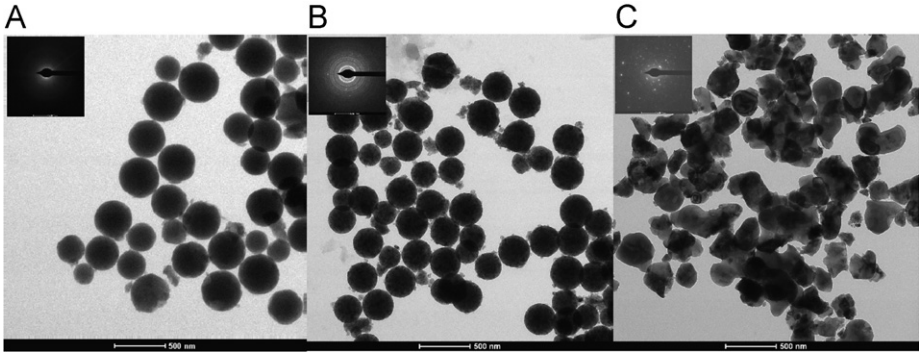

Fig. 1. TEM images of TiO_2 nanoparticles with different crystal styles (A) amorphous, (B) anatase and (C) rutile.

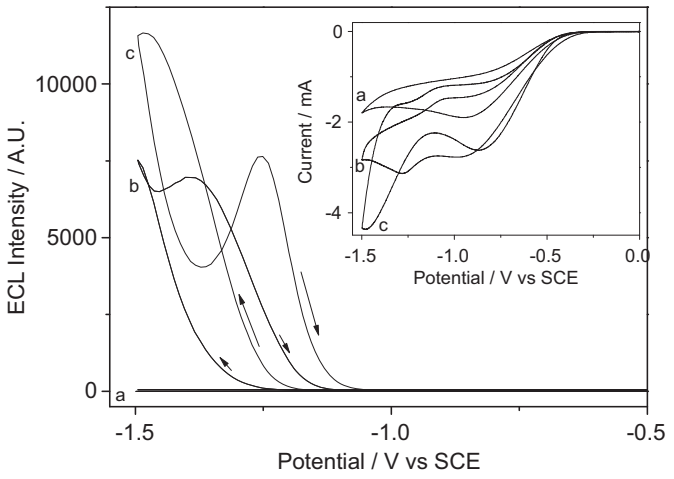

Fig. 2. ECL intensity-potential curves of TiO_2 nanoparticles with three crystal styles: (a) amorphous; (b) anatase and (c) rutile in 0.1 M PBS (pH 9) containing 10 mM H_2O_2 with the scan rate of 100 mV s^{-1}. Insert: corresponding cyclic voltammgramms.

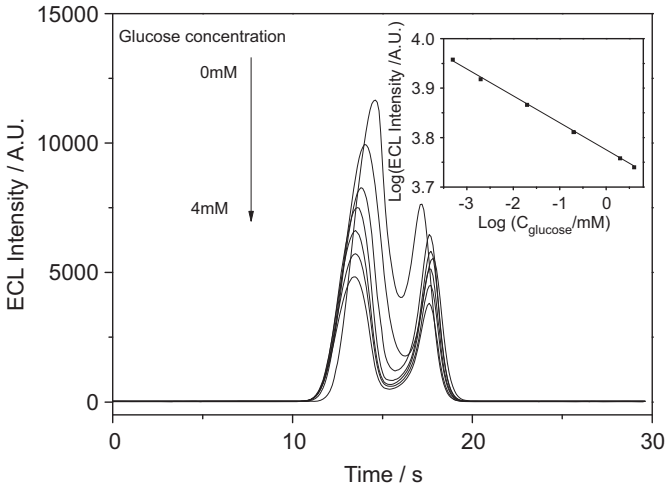

Fig. 3. Variation in the ECL Intensity of the Au seeds-TiO_2 on FTO upon treatment with the growth solution of different concentrations of glucose: (a) 0 M; (b) 5×10^{-7} M; (c) 2×10^{-6} M; (d) 2×10^{-5} M; (e) 2×10^{-4} M; (f) 2×10^{-3} M and (g) 4×10^{-3} M from the top down. Inset: logarithmic calibration curve of the prepared glucose biosensor.

which is due to electron injection into rutile TiO_2 to produce the reduced TiO_2 form in the cathodic process (Curve a in the inset of Fig. S1). Meanwhile, no ECL was monitored in the process (Curve a in Fig. S1) due to the absence of co-reactant. In the saturated oxygen and 10 mM H_2O_2 solution, the cathodic currents increase for the reduction of oxygen and H_2O_2, and the electron injected into TiO_2 nanocrystals are also observed beyond -1.0 V with the decrease of the oxidative current of the reduced TiO_2 NCs (Curve b and c in the inset of Fig. S1), the ECL intensity occurs beyond -1.0 V which consists with the voltage onset of electron injection (Curve b and c in Fig. S1).

3.2. ECL quenching effect by gold nanoparticles

Gold nanoparticles (Au-NPs) were introduced onto the surface of TiO_2 via the bi-linking reagent, 3-mercaptopropionic acid (MPA). $TiO_{2\ rutile}$/FTO was immersed into 1 mM MPA solution for 30 min to assemble MPA via –COOH. The adsorbed MPA monolayer was used to anchor nanogold via thiol-Au bond. As shown in Fig. S2 in the supplemental information, the introduction of nanogold induced the decrease of the ECL intensity due to the energy transfer (Shan et al., 2009). Subsequently, the seeded Au NPs-TiO_2 hybrid film was allowed to incubate for 5 min at 30 °C in a growth solution of 0.01 M PBS (pH 7.0) containing 2.4×10^{-4} M $HAuCl_4$, 2×10^{-3} M cetyltrimethylammonium chloride (CTAC) and H_2O_2 with various concentrations. The enlargement process of Au NP seeds upon the H_2O_2 treatment was tracked by UV–vis absorbance spectra. Fig. S3 in the supplemental information shows the evolution of the absorbance spectra of the Au NPs-TiO_2 film and it is clearly characterized by the localized surface plasmon resonance (LSPR) peak of Au NPs. As the H_2O_2 concentration increases, the absorbance corresponding to the LSPR of Au NPs intensifies, indicating the increase of Au loading on the film.

3.3. Detection of glucose

The catalytic growth of Au NP seeds and the quenching of ECL of TiO_2 are directly related to the H_2O_2 concentration. So, by monitoring the changes of the ECL intensity after the specific biocatalytic reaction which could produce H_2O_2, a new ECL biosensor could be tailored. Glucose oxidase (GOD) and glucose were then chosen and tested for the determination of glucose. GOD catalyzes the oxidation of glucose to generate H_2O_2 for the reduction of the $HAuCl_4$ under the catalysis of seeded Au NPs. The concentration of the generated H_2O_2 rises with the increase of glucose concentration, leading to the increase in Au NPs loading. The seeded Au NPs-TiO_2 hybrid films are immersed in the growth solution of $AuCl_4^-$ salt and GOD in the presence of variable concentrations of glucose for 15 min at 30 °C and then the ECL intensity was recorded.

Fig. 3 displays the resulting ECL intensity vs. time plots and the inset shows the corresponding derived calibration curve. During this measure period, voltage cyclically scanned from 0 to -1.5 V, then, came back to 0 V at a scan rate of 100 mV s^{-1}. The two peaks of ECL each curve appeared corresponding to the voltage scanning forward and backward processes, respectively. The chemical reactions involved listed as follows:

$$TiO_{2\ rutile} + e^- \rightarrow TiO_{2\ rutile}(e^-) \quad (1)$$

$$2TiO_{2\ rutile}(e^-) + H_2O_2 \rightarrow TiO_{2\ rutile}^{*} + 2OH^- \quad (2)$$

$$TiO_{2\ rutile}^{*} \rightarrow TiO_2 + h\nu \quad (3)$$

The ECL intensity decreases as the concentration of glucose increases, indicating the glucose controlled growth of Au NPs. The inset shows the linear logarithmic calibration plot for glucose detection. In the range 5×10^{-7}–4.0×10^{-3} M, the ECL intensity decreased linearly. The limit of detection was 2.5×10^{-7} M. The ECL quenching by biological enlarged nanogold particles to detect 1.0×10^{-5} M glucose for five nanogold seeds-$TiO_{2\ rutile}$/FTOs fabricated independently showed the relative standard deviation (RSD) of 4.8%, giving an acceptable assay reproducibility of the method.

4. Conclusion

Three kinds of TiO_2 nanoparticles, amphorous, antanase and rutile were facilely prepared. The ECL properties were observed only in crystal TiO_2 film. Interestingly, gold nanoparticles were found to quench the ECL of TiO_2 nanocrystals in H_2O_2 solution. Nanogold seeds adsorbed on the surface of TiO_2 NCs can grow up in $HAuCl_6$ solution with the biologically generated H_2O_2 via a GOD bio-catalyzing glucose system as a model in ambient condition.

The quenching effect enhances linearly with the enlargement of nanogold, which was related to the biological produced H_2O_2, then glucose. Therefore, a sensitive ECL biosensing platform to detect glucose was fabricated based on the above quenching mechanism. Apparently, the protocol to fabricate ECL biosensors is also suitable to other biologically produced H_2O_2 or NADH bio-systems. It is expected that the promising properties of such ECL biosensing concept may be useful for the development of immunosensors or DNA and protein sensors involving a target labeled by an oxidase.

Acknowledgments

We acknowledge the financial support of this work by the Natural Science Foundation of China (Nos. 20905011, 21010102071, 21175114), the Natural Science Foundation of Jiangsu (No. BK2010396), the Scientific Research Foundation for the returned overseas Chinese scholars, MOE, the Open Research Fund of State Key Laboratory of Bioelectronics, Southeast University, and the Southeast University Creative Foundation (3207040501).

Appendix A. Supporting information

Supplementary data associated with this article can be found in the online version at http://dx.doi.org/10.1016/j.bios.2012.07.065.

References

Bruchez, M., Moronne, M., Gin, P., Weiss, S., Alivisatos, A.P., 1998. Science 281, 2013–2016.
Bae, Y., Myung, N., Bard, A.J., 2004. Nano Letters 4, 1153–1161.
Chan, W.C.W., Nie, S.M., 1998. Science 281, 2016–2018.
Chen, L., Xu, N., Yang, H., Zhou, C., Chi, Y., 2011. Electrochimica Acta 56, 1387–1391.
Ding, S.N., Xu, J.J., Chen, H.Y., 2006. Chemical Communications 34, 3631–3633.
Ding, Z., Quinn, B.M., Haram, S.K., Pell, L.E., Korgel, B.A., Bard, A.J., 2002. Science 296, 1293–1297.
Ding, S.N., Xu, J.J., Shan, D., Gao, B.H., Yang, H.X., Sun, Y.M., Cosnier, S., 2010. Electrochemistry Communications 12, 713–716.
Diez, I., Pusa, M., Kulmala, S., Jiang, H., Walther, A., Goldmann, A.S., Muller, A.H.E., Ikkala, O., Ras, R.H.A., 2009. Angewandte Chemie International Edition 48, 2122–2125.
Geng, J., Liu, B., Xu, L., Hu, F.N., Zhu, J.J., 2007. Langmuir 23, 10286–10293.
Liu, X., Jiang, H., Lei, J., Ju, H., 2007. Analytical Chemistry 79, 8055–8060.
Li, L., Liu, H., Shen, Y., Zhang, J., Zhu, J., 2011. Analytical Chemistry 83, 661–665.
Lin, Z., Liu, Y., Chen, G., 2008. Electrochemistry Communications 10, 1629–1632.
Li, J., Yang, L., Luo, S., Chen, B., Li, J., Lin, H., Cai, Q., Yao, S., 2010. Analytical Chemistry 82, 7357–7361.
Liu, X., Hou, Z., Lei, J., Ju, H., Cai, J., Shen, J., 2011. Electroanalysis 23, 2629–2632.
Myung, N., Ding, Z., Bard, A.J., 2002. Nano Letters 2, 1315–1319.
Myung, N., Lu, X., Johnston, K.P., Bard, A.J., 2004. Nano Letters 4, 183–185.
Poznyak, S.K., Talapin, D.V., Shevchenko, E.V., Weller, H., 2004. Nano Letters 4, 693–698.
Pavlov, V., Xiao, Y., Willner, I., 2005. Nano Letters 5, 649–653.
Shan, Y., Xu, J.J., Chen, H.Y., 2009. Chemical Communications, 905–907.
Shan, Y., Xu, J.J., Chen, H.Y., 2010a. Chemical Communications 46, 4187–4189.
Shan, Y., Xu, J.J., Chen, H.Y., 2010b. Chemical Communications 46, 5079–5081.
Shlyahovsky, B., Katz, E., Xiao, Y., Pavlov, V., Willner, I., 2005. Small 1, 213–216.
Tanaka, S., Nogami, D., Tsuda, N., Miyake, Y., 2009. Journal of Colloid and Interface Science 334, 188–194.
Wu, M.S., Shi, H.W., Xu, J.J., Chen, H.Y., 2011. Chemical Communications 47, 7752–7754.
Xiao, Y., Pavlov, V., Levine, S., Niazov, T., Markovitch, G., Willner, I., 2004. Angewandte Chemie International Edition 43, 4519–4522.
Zou, G., Ju, H., 2004. Analytical Chemistry 76, 6871–6876.
Zheng, L., Chi, Y., Dong, Y., Lin, J., Wang, B., 2009. Journal of the American Chemical Society 131, 4564–4565.
Zhang, R., Fan, L., Fang, Y., Yang, S., 2008. Journal of Materials Chemistry 18, 4964–4970.
Zayats, M., Baron, R., Popov, I., Willner, I., 2005. Nano Letters 5, 21–25.